ARMY RESEARCH LABORATORY

Parallel/Oblique Impact on Thin Explosive Samples

Vincent M. Boyle
Robert B. Frey
Alfred L. Bines

ARL-TR-584 October 1994

NOTICES

Destroy this report when it is no longer needed. DO NOT return it to the originator.

Additional copies of this report may be obtained from the National Technical Information Service, U.S. Department of Commerce, 5285 Port Royal Road, Springfield, VA 22161.

The findings of this report are not to be construed as an official Department of the Army position, unless so designated by other authorized documents.

The use of trade names or manufacturers' names in this report does not constitute indorsement of any commercial product.

REPORT DOCUMENTATION PAGE

Form Approved
OMB No. 0704-0188

1. AGENCY USE ONLY (Leave blank)	2. REPORT DATE	3. REPORT TYPE AND DATES COVERED
	October 1994	Final, 1 Jan 90 30 Sep 92

4. TITLE AND SUBTITLE

Parallel/Oblique Impact on Thin Explosive Samples

5. FUNDING NUMBERS

PR: 1L161102AH43

6. AUTHOR(S)

Vincent M. Boyle, Robert B. Frey, and Alfred L. Russ

7. PERFORMING ORGANIZATION NAME(S) AND ADDRESS(ES)

U.S. Army Research Laboratory
ATTN: AMSRL-WT-TB
Aberdeen Proving Ground, MD 21005-5066

8. PERFORMING ORGANIZATION REPORT NUMBER

9. SPONSORING/MONITORING AGENCY NAME(S) AND ADDRESS(ES)

U.S. Army Research Laboratory
ATTN: AMSRL-OP-AP-L
Aberdeen Proving Ground, MD 21005-5066

10. SPONSORING/MONITORING AGENCY REPORT NUMBER

ARL-TR-304

11. SUPPLEMENTARY NOTES

12a. DISTRIBUTION/AVAILABILITY STATEMENT

Approved for public release; distribution is unlimited.

12b. DISTRIBUTION CODE

13. ABSTRACT (Maximum 200 words)

Parallel/oblique impact experiments were conducted on thin (0.6 mm - 1.0 mm) explosive samples in order to induce a well defined state of combined pressure and shear in the sample. A compressed gas gun accelerated a projectile which impacted the thin explosive sample over a 130 mm diameter. The impacted explosive was viewed by a high speed framing camera through a transparent anvil in order to detect evidence of reaction. Simplified assumptions were made in order to calculate the pressure and the strain rate; the pressure range of these experiments was from 0.5 GPa to 1.31 GPa, and the strain rate across the sample was 30,000 per second assuming a viscosity of 30,000 poise. No explosive reaction was detected for the 15 μs duration of these tests. The temperature due to viscoplastic heating of the explosive was calculated for several explosive thicknesses, viscosities and yield strengths, and several projectile impact velocities. Using reasonable values of viscosity and yield strength, the maximum temperature increase for these tests was calculated to be 91 °C. The limitations of this experiment and possible improvements are discussed.

14. SUBJECT TERMS

explosive ignition, pressure-shear ignition, shear band, viscous heating, compressed gas guns, shear tests, strain rate

15. NUMBER OF PAGES

30

16. PRICE CODE

17. SECURITY CLASSIFICATION OF REPORT	18. SECURITY CLASSIFICATION OF THIS PAGE	19. SECURITY CLASSIFICATION OF ABSTRACT	20. LIMITATION OF ABSTRACT
UNCLASSIFIED	UNCLASSIFIED	UNCLASSIFIED	UL

INTENTIONALLY LEFT BLANK.

TABLE OF CONTENTS

INTENTIONALLY LEFT BLANK.

LIST OF FIGURES

INTENTIONALLY LEFT BLANK.

LIST OF TABLES

INTENTIONALLY LEFT BLANK.

1. INTRODUCTION

The shearing of explosive materials under pressure is an effective way to produce localized heating by viscoplastic work concentrated in a small region of the deforming explosive. This localized heating can cause the explosive to react releasing additional heat to accelerate the reaction. In an earlier paper, we described the results obtained when a small cylinder of explosive was pressurized within heavy steel confinement and then allowed to slide against the steel confinement (Boyle, Frey, and Blake 1989); in a similar arrangement, we investigated explosive on explosive shear by punching a plug from the pressurized explosive cylinder. In those experiments, we demonstrated that the ignition threshold depends on both pressure and shear velocity. Those experiments had a relatively long duration of about 1 ms, a maximum pressure of about 1.0 GPa, and a maximum shearing velocity of about 80 m/s; the pressure and shear velocity varied during the course of the experiment. The rise time to peak pressure was several hundred μs. Also the shear localization was not well defined so the local strain rate could not be determined. In the experiments reported here, we have attempted to study the ignition of several explosives as they were impacted under conditions that would cause the explosive sample to shear in a known manner under the high pressure of the impact. A maximum pressure of 1.3 GPa was reached with a strain rate of about 50,000 per second over an explosive layer 0.6 mm thick.

2. EXPERIMENTAL APPROACH

In order to obtain well-defined conditions for pressure-shear impact on explosive, we adapted a technique described by Abou-Sayed, Clifton, and Hermann (1976), Kim and Clifton (1980), and Li and Clifton (1981). In this technique, one-dimensional combined pressure shear waves were generated in a flat target plate by the impact of a flat, high acoustic impedance flyer plate; both the flyer plate and the target plate were inclined at an angle to the velocity vector of the flyer plate in order to produce a shear component of particle velocity in the impacted target. The impact occurred simultaneously at all points of the flyer-target interface. In addition, a high acoustic impedance anvil supported the target plate. The flyer plate and anvil have higher acoustic impedance than the target plate in order to prevent unloading of the target by reflection of waves at the target interfaces. This arrangement is illustrated in Figure 1 for the flyer plate impacting a target at 30° obliquity. A gas gun was used to accelerate the flyer plate. Details of the gas gun and projectile are shown in Appendix A. From Figure 1, it can be seen that the flyer plate velocity has a component normal to the target plate, V_n, and a component parallel to the target plate, V_t. These components can be calculated as follows:

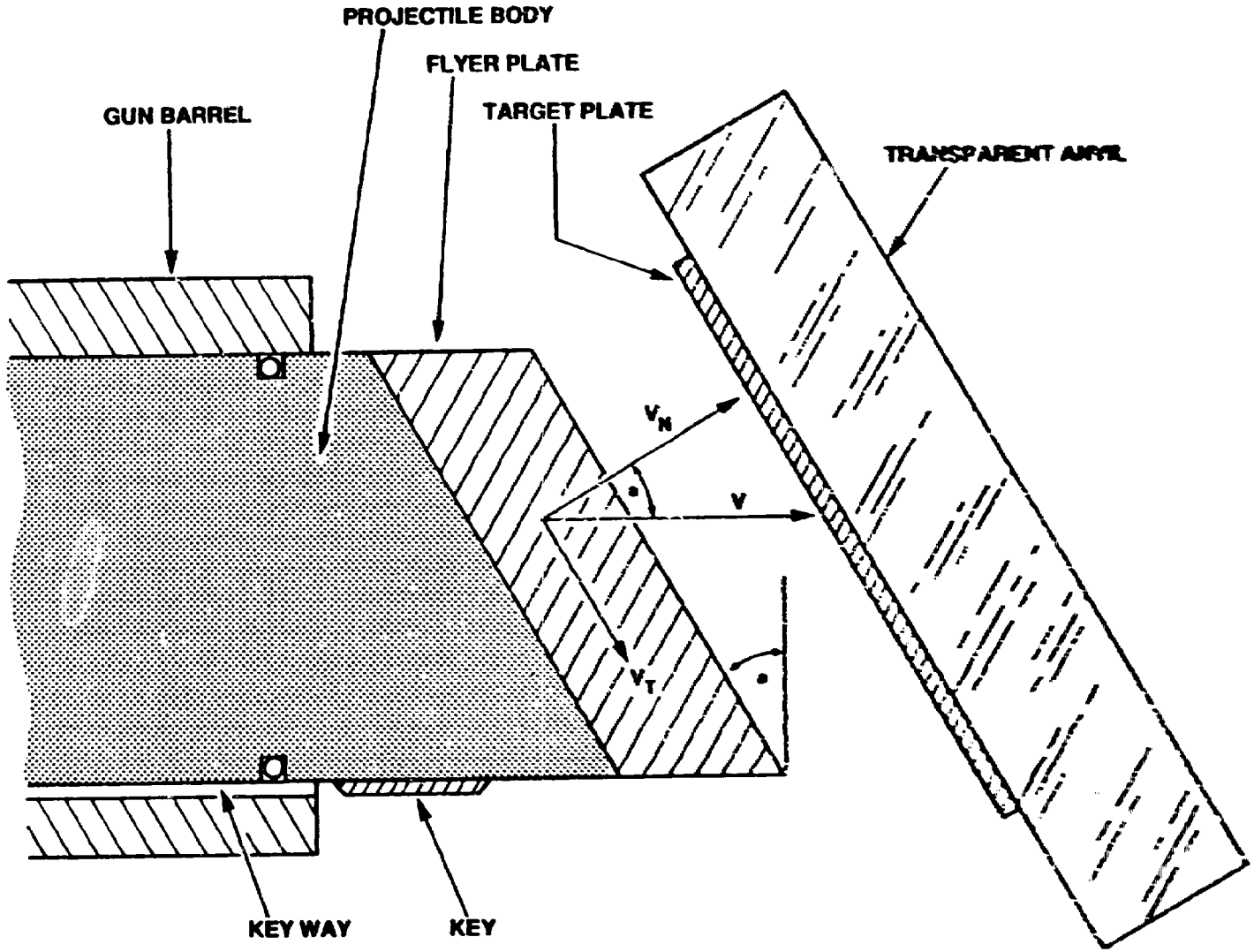

Figure 1. Parallel/oblique impact of a flyer plate on a thin explosive sample. The normal and tangential components of the flyer plate before impact are illustrated.

$$V_n = V (\cos a) , \quad (1)$$

and

$$V_t = V (\sin a) , \quad (2)$$

where V is the flyer plate velocity and a is the angle of obliquity of the flyer plate with respect to the target plate (the angle between the flyer plate velocity and the normal to the target plate). Upon impact, the normal component of the flyer plate velocity generates a stress wave in the target; this stress wave is reflected between the high impedance boundaries several times until the target reaches a state of uniform stress determined by the flyer plate velocity and the material properties of the flyer plate, target plate, and anvil. Likewise, the parallel component of flyer plate velocity, by its traction with the target surface, produces a shear wave in the target which, after several reverberations, induces a state of uniform shear. The strain rate associated with this shear is determined by the parallel component of flyer plate velocity; the material properties of the flyer plate, target plate, and anvil; and the thickness of the target plate.

A high speed framing camera, Cordin Model 192, was operated at half speed, 2,500 rps, in its rotary-prism mode in order to record the impact of the flyer plate on the explosive target; this impact was viewed through a 50 mm-thick transparent anvil. The camera records 80 frames, and the interframe time at this speed is approximately 1.7 μs. However, we were usually limited to about 15 μs of observation after impact because the free surface of the anvil became opaque shortly after the elastic wave arrived there. Two explosive light sources (argon bombs) were used to illuminate the explosive surface being viewed by the camera. The argon bombs consisted of a volume of argon gas inside a conical cardboard container with an aluminized, reflecting inner surface; the container was sealed at the larger end by a transparent window of Saran Wrap. A 300-g Comp B explosive charge was taped inside the smaller end. When the explosive charge is detonated, a strong shock wave is produced in the argon causing it to luminesce and emit high intensity light as the shock wave progresses through the argon. For the 600 mm long argon bombs used in these tests, we had sufficient light to record for approximately 60 μs.

These tests were done inside a blast chamber. The compressed gas gun was mounted on a mobile cart so it could be removed from the chamber when necessary, Figure 2. In practice, we ended up welding the cart in place in order to obtain a more rigid structure and improve the simultaneity of impact. An aluminum frame with several degrees of freedom was used to hold the anvil and explosive target and align them with the face of the projectile. A rag-filled catcher tank was used to catch the projectile and some of the target debris. The experimental arrangement is shown in Figure 3.

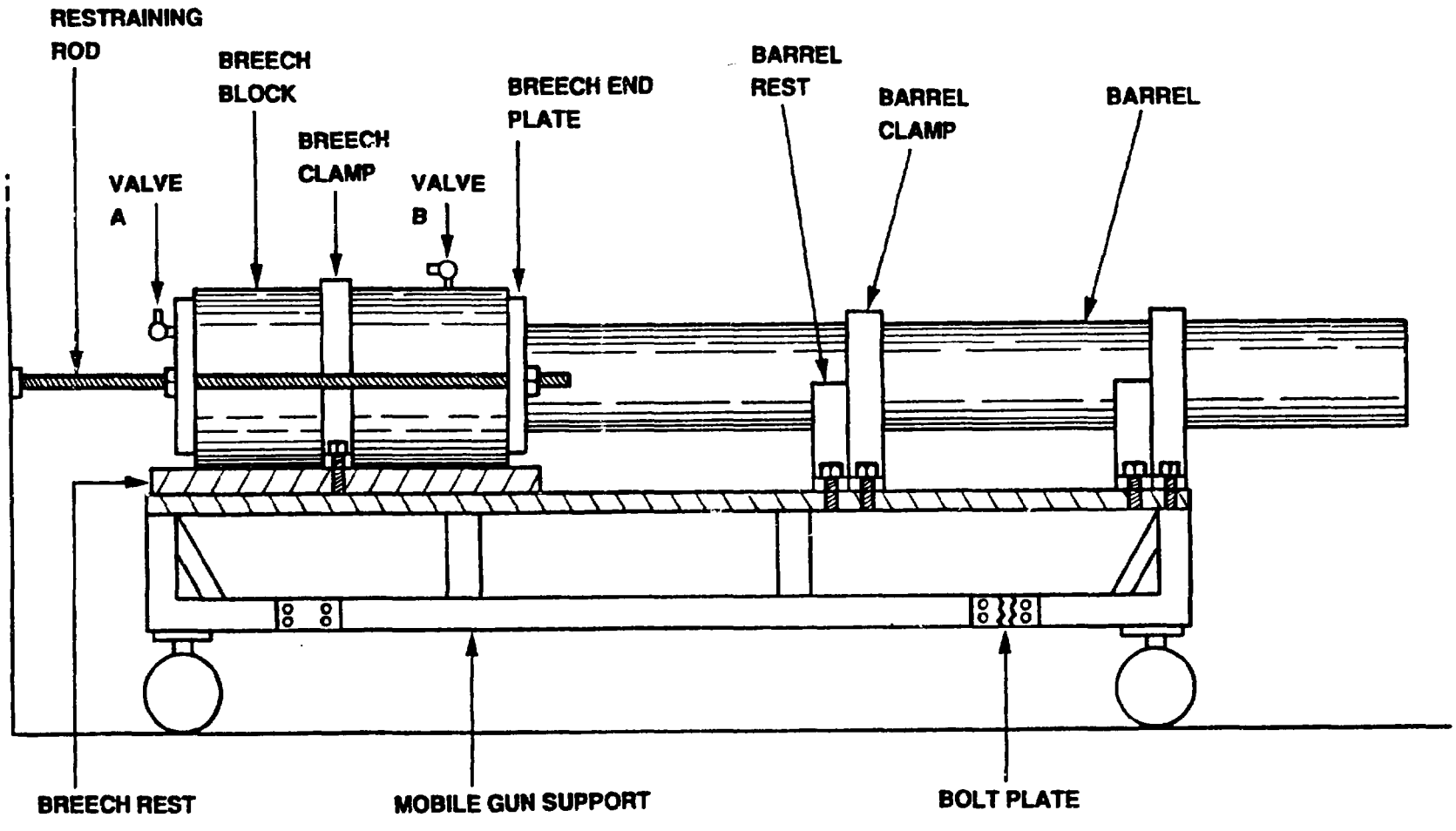

Figure 2. The compressed gas gun is shown mounted on its mobile cart. This arrangement was used to wheel the gun into the blast chamber.

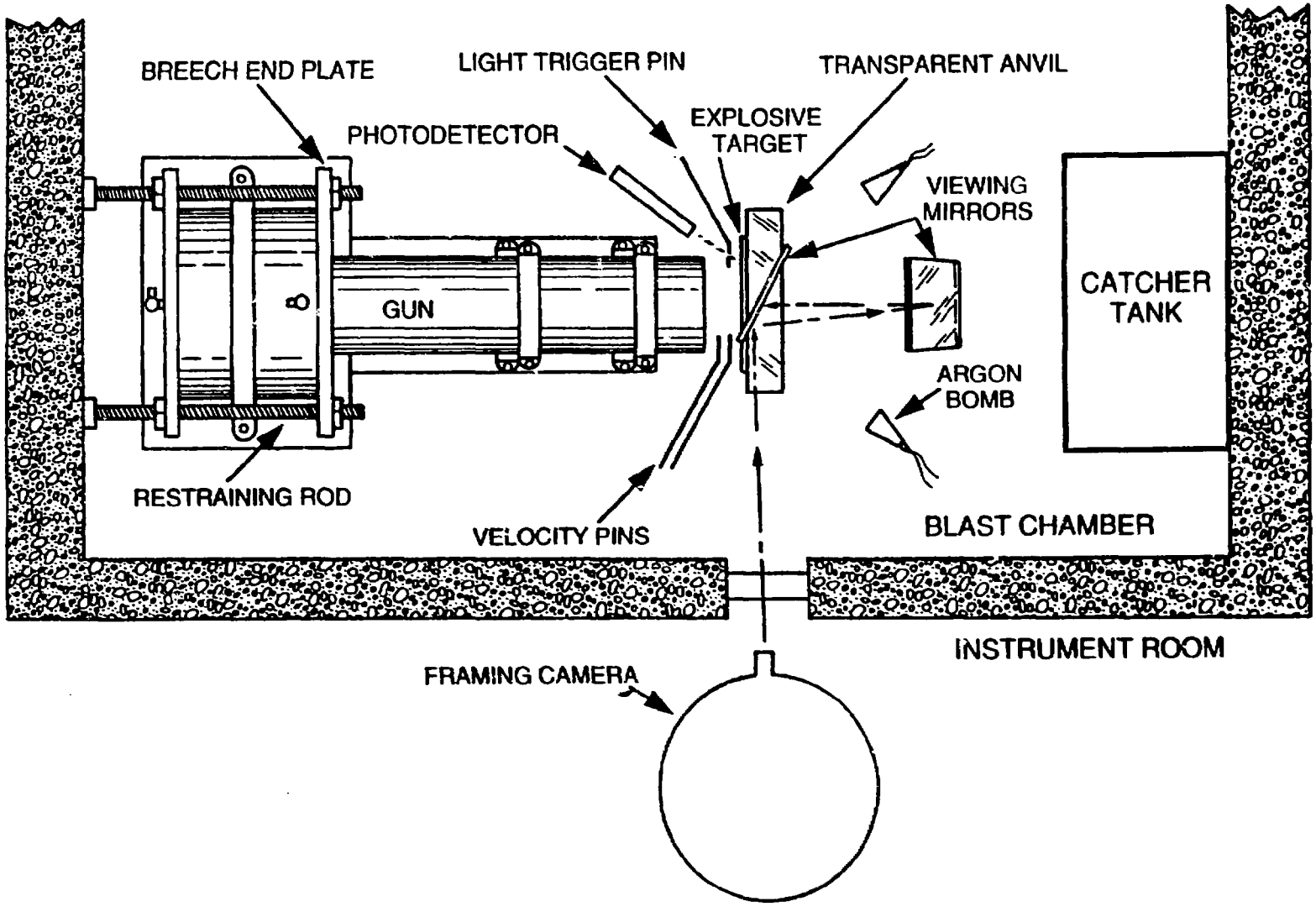

Figure 3. An overall view of the experimental arrangement.

In the experiments reported here, the strain rate in the explosive target can be calculated as

$$(V_{tp} - V_{ta}) / x , \tag{3}$$

where V_{tp} and V_{ta} are the components of the projectile velocity and the anvil velocity parallel to the interface after impact and x is the original thickness of the explosive sample. This calculation is shown in Appendix B.

In order to calculate the stress in the explosive sample, we assumed that the flyer plate and the anvil remained elastic during the impact and, after several reverberations, the explosive attained a stress level equal to what would be achieved by the impact of the flyer plate directly on the anvil. With these assumptions and the requirement that the particle velocity and pressure remain equal at the flyer plate-anvil interface, we were able to calculate the stress in the explosive. For a steel flyer plate and a glass anvil, the pressure in the explosive can be calculated (see Appendix C):

$$P_x = (\rho_f U_f) (\rho_a U_a) V_n / (\rho_f U_f + \rho_a U_a) , \tag{4}$$

where

P_x is the pressure in the explosive sample, dynes/cm^2
(10^{10} dynes/cm^2 = 1 GPa = 10 kbars)
ρ_f is density of the flyer plate, g/cm^3
ρ_a is density of the anvil, g/cm^3
V_n is the normal component of flyer plate velocity, cm/s
U_f is the elastic wave velocity in the flyer plate, cm/s
U_a is the elastic wave velocity in the anvil, cm/s.

Table 1 lists the relevant material properties for the flyer plates and anvils described in this report.

Table 2 lists the experimental data for the tests which are being reported here.

Using the data from Table 2, we were able to calculate the strain rate (Appendix B) and pressure (Appendix C) in the explosive sample. These values, as well as the impact simultaneity along the projectile/target interface, are listed in Table 3. We should comment that the calculated strain rate depends on the value assumed for viscosity. The effect of changing the viscosity is shown in Appendix B.

Table 1. Material Properties of Flyer Plates and Anvils

Material	Density (g/cm^3)	Elastic Wave Velocity (cm/s)
steel, 1020	7.89	5.96×10^5
aluminum, 2024-T4	2.78	6.30×10^5
glass[a]	2.23	5.64×10^5
Plexiglas	1.18	2.70×10^5

[a] The glass, a water white borosilicate, was used as an anvil; it was actually a laminate consisting of four glass and three plastic plies. The overall thickness was 2 in, and the individual glass plies were 0.5 in thick. The plastic plies were polyvinyl butyryl, 0.015 in thick.

Table 2. Experimental Data for Tests

Shot No.	Flyer Plate	Flyer Plate Velocity (m/s)	Explosive Sample	Anvil
1	flat, aluminum	147	1-mm TNT	Plexiglas
2	flat, aluminum	148	1-mm TNT	Plexiglas
3	flat, aluminum	174	1-mm TNT	Plexiglas
4	angled, aluminum	—	1-mm TNT	Plexiglas
5	angled, aluminum	148	1-mm DS	Plexiglas
6	flat, steel	132	1-mm DS	glass
7	flat, steel	125	1-mm DS	glass
8	angled, steel	125	1-mm DS	glass
9	angled, steel	145	1-mm DS	glass
10	flat, steel	—	1-mm DS	glass
11	angled, steel	153	1-mm DS	glass
12	flat, steel	143	1-mm DS	glass

NOTE: DS = Detasheet is an explosive made by the DuPont Company; it contains 63% by weight PETN, 8% nitrocellulose, and 29% acetyltributylcitrate. Its density was about 1.48 g/cm^3.
TNT = cast TNT of density 1.60 g/cm^3.

Table 2. Experimental Data for Tests (continued)

Shot No.	Flyer Plate	Flyer Plate Velocity (m/s)	Explosive Sample	Anvil
13	flat, steel	144	1-mm DS	glass
14	angled, steel	148	1-mm DS	glass
15	angled, steel	143	1-mm DS	glass
16	angled, steel	—	1-mm DS	glass
17	angled, steel	—	1-mm DS	glass
18	angled, steel	120	1-mm DS	glass
19	flat, steel	127	1-mm DS	glass
20	flat, steel	79	1-mm DS	glass
21	flat, steel	89	1-mm DS	glass
22	flat, steel	57	1-mm DS	glass
23	flat, steel	58	1-mm DS	glass
24	flat, steel	103	1-mm DS	glass
25	flat, steel	69	0.5-mm Pent.	glass
26	angled, steel	153	0.6-mm DS	glass
27	flat, steel	64	0.6-mm DS	glass
28	angled, steel	42	0.6-mm DS	glass
29	angled, steel	39	0.6-mm DS	glass
30	angled, steel	59	0.6-mm DS	glass

NOTE: DS = Detasheet is an explosive made by the DuPont Company; it contains 63% by weight PETN, 8% nitrocellulose and 29% acetyltributylcitrate. Its density was about 1.48 g/cm^3.
Pent. = cast Pentolite (50% PETN/50% TNT) of density 1.67 g/cm^3.

Table 3. Pressure, Strain Rate of Explosive, and Impact Simultaneity

Shot No.	Pressure (GPa)	Strain Rate[a] (1/s)	Impact Simultaneity (μs)
1	0.39	0	—
2	0.40	0	—
3	0.47	0	12
4	—	—	—
5	0.35	35,000	
6	1.31	0	—
7	1.24	0	15
8	1.07	31,000	—
9	1.25	36,000	—
10	—	—	—
11	1.31	38,000	20
12	1.42	0	—
13	1.43	0	2
14	1.27	37,000	10
15	1.23	36,000	10
16	—	—	—
17	—	—	—
18	1.03	29,000	3
19	1.26	0	0
20	0.78	0	—
21	0.88	0	0
22	0.56	0	—
23	0.57	0	2

[a] This is for the strain rate calculated assuming a viscosity of 50,000 poise and a yield strength of 0.35×10^9 dynes/cm^2 for Detasheet.

Table 3. Pressure, Strain Rate of Explosive, and Impact Simultaneity (continued)

Shot No.	Pressure (GPa)	Strain Rate[a] (1/s)	Impact Simultaneity (μs)
24	1.02	0	5
25	0.68	0	4
26	1.31	49,000	10
27	0.63	0	8
28[b]	0.36	10,000	7
29[b]	0.33	9,600	—
30	0.51	17,000	—

[a] This is the strain rate calculated assuming a viscosity of 50,000 poise and a yield strength of 0.35×10^9 dynes/cm^2 for Detasheet.

[b] For these shots, an IR detector monitored a small region of explosive at the edge of the impact zone.

The dash lines in Table 2 indicate an absence of data due to failure of the arrival time circuitry used to measure projectile velocity.

In Table 3, the dash lines indicate a lack of data for various reasons; failure of the velocity pin circuitry, malfunctioning of the framing camera shutter or mistiming of the explosive light source used to illuminate the explosive target.

3. RESULTS

As can be seen from the data in Table 3, many of our tests did not have good impact simultaneity of the flyer plate on the surface of the explosive target. Also, in many of the tests, we were not able to observe the impact, due to experimental problems. For the impacts that we were able to observe, we did not see any obvious sign of explosive reaction such as light emission or the expulsion of reaction products from the region of impact. In all cases, the explosive in the impacted region became darker in about 4–6 μs; after this, the darkness did not appear to increase during the available time of observation, about 15 μs. However the darkness did appear to increase with the impact pressure. For some of the shots (No. 14 vs. No. 19 and No. 18 vs. No. 24), we were able to compare shear and nonshear tests at pressures which were nearly equal; the presence or absence of shear did not appear to have an effect on explosive darkening.

For shot No. 25, the explosive target consisted of a 0.5-mm cast sheet of Pentolite explosive in which the grain boundaries were very prominent. Upon impact at 0.68 GPa the grain boundaries were noticeably darker than the rest of the explosive for several microseconds and then the entire impacted region became uniformly dark.

Since we were not able to tell if the explosive darkening meant that reaction was occurring, we tried to detect IR radiation by using a photovoltaic silicon photodiode that was sensitive to wavelengths from the visible to the near IR (300 nm to 1,100 nm). Two longpass IR filters were used in tandem in front of the photodiode in order to attenuate the visible light from the argon bombs by a factor of 10 billion; the cut on wavelength was 785 nm. The filters and photodetector were shielded from stray light by enclosing them within a phenolic tube which was pointed toward the impacted surface of the explosive sample as shown in Figure 3. The photodetector viewed a small region on the edge of the impact area. For shot No. 29, the argon bombs did not function and the photodiode did not detect any signal during 6 ms of observation. For shot No. 30, the argon bombs functioned and the photodiode detected a signal but it corresponded to the turn on of light from the argon bombs before the flyer plate even impacted the explosive target.

Several shots were fired for which the rear surface (the surface facing the camera) of the explosive was marked beforehand with fine lines using a permanent marker. The lines appeared to remain undistorted during the time of observation, even though the impacted area of the explosive became dark. This was true even at an impact pressure of 1.02 GPa, shot No. 24.

Examination of the debris recovered after the shot did not reveal any evidence of explosive reaction having occurred. The flyer plate did not have any carbon residue or other indications of explosive reaction. The explosive within the impact zone was broken into small irregular fragments. The anvil was generally shattered into many small pieces. The projectile and most of the debris from the impact zone ended up embedded in the rags within the catcher tank.

4. DISCUSSION

We were surprised that we were unable to detect any obvious sign of explosive reaction for Detasheet since, in the paper previously mentioned (Boyle, Frey, and Blake 1989), we were able to cause Detasheet to react under what appeared to be a milder stimulus, 0.2-GPa pressure and a shear velocity of 60 m/s.

The duration of those tests was about 500 μs, whereas the tests reported here would be terminated when release waves originating at the boundary of the flyer plate reached the axis, a time of about 15 μs. The longer duration of those earlier tests may have allowed the explosive to reach temperatures required for reaction. Also, in those earlier tests a cylinder of explosive was slid along a boundary of either steel or explosive causing the explosive temperature to increase due to viscoplastic heating. The shear may have become more localized in those earlier tests due to greater thermal softening of the explosive at the peak temperature region within the shear band. The concentration of shear motion in a narrow region would increase the strain rate and the peak temperature.

In our current tests, if the strain rate is uniform across the target plate, the temperature increase in the target plate can be expressed by the formula,

$$\Delta T = (\nu\,[d\varepsilon/dt]^2 + Y\,[d\varepsilon/dt]\,)\,t/\rho c\,, \qquad (5)$$

where

ΔT = temperature increase (°C)
ν = viscosity (poise)
$d\varepsilon/dt$ = strain rate (1/s)
t = time duration (s)
ρ = density (g/cm^3)
c = specific heat (ergs/g-°C)
Y = yield stress in shear (dynes/cm^2).

For the experiments reported here, the strain rate of the explosive is a function of its thickness, viscosity, and yield strength, as well as the component of the flyer plate velocity parallel to the explosive surface, and the material properties of the flyer plate and anvil; this relationship is indicated in equations B4–B10 in Appendix B. Using this relationship, we computed the strain rates corresponding to a range of explosive viscosities and yield strengths for shot No. 26. We then used equation 5 to calculate the corresponding temperature increase, assuming a time duration of 15 μs, an explosive density of 1.48 g/cm^3, and a specific heat of 1.25×10^7 ergs/g-°C. Figure 4 shows the temperature increase in the explosive target as a function of its viscosity and yield strength. It can be seen that the calculated temperature increase, over a wide range of viscosity and yield strength, is no greater than 116° C. We would not expect to see evidence of explosive reaction in our experiment at such a low temperature.

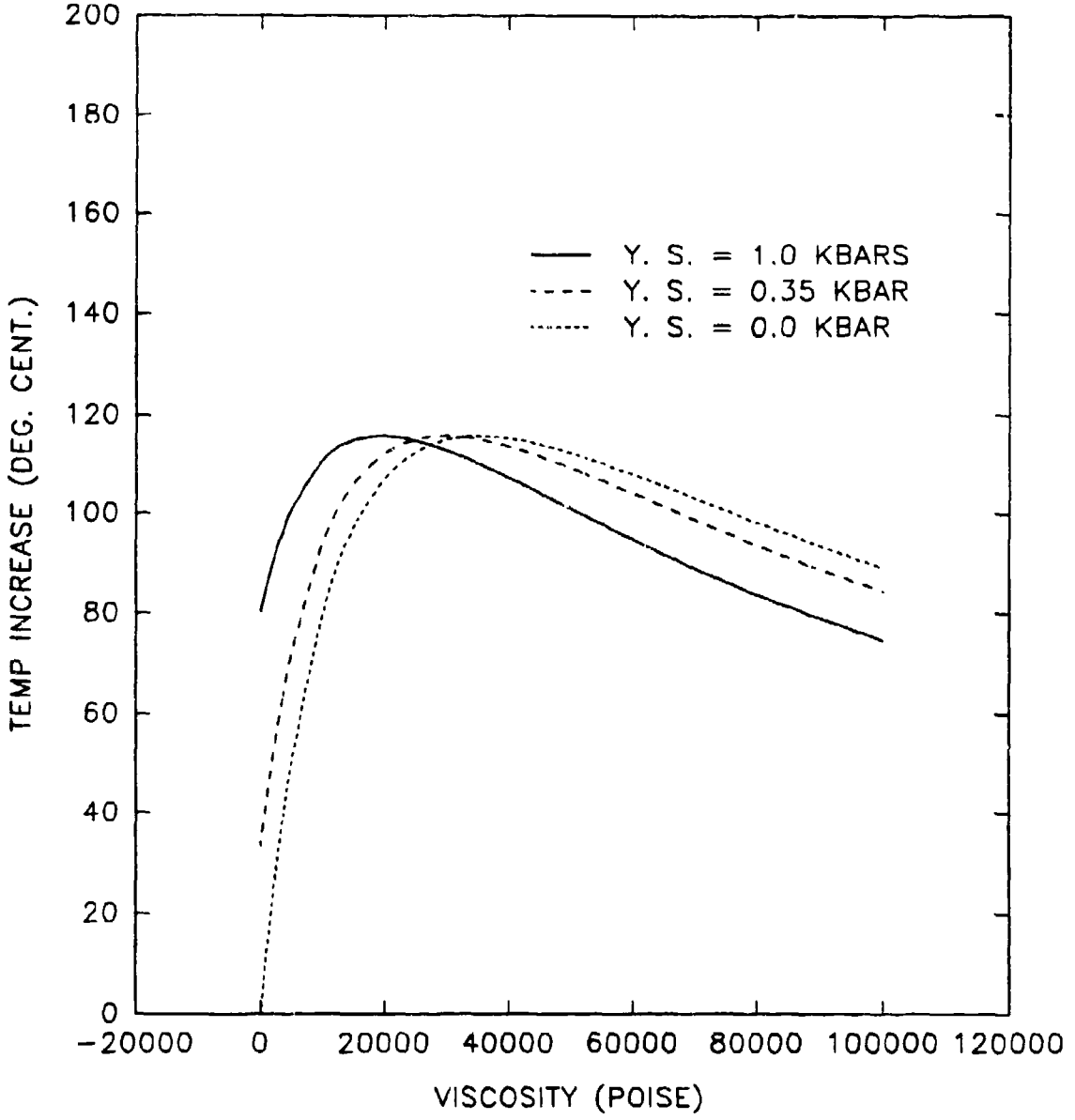

Figure 4. The temperature increase in an explosive target plotted as a function of viscosity and yield strength of the explosive. The sample thickness is 0.06 cm, and the transverse component of the flyer plate velocity is 7,650 cm/s.

We can use Frank-Kamentskii's equation for the adiabatic explosion time (AMCP 706-180, 1972) to calculate the temperature required to produce a thermal explosion in 15 μs. We used the following data for PETN (Rogers 1975) for the required input parameters:

Specific heat	1.25×10^7 ergs/g-°C
Gas constant	8.31×10^7 ergs/g-mol-°C
Early heat of reaction	1.26×10^{10} ergs/g
Frequency factor	6.3×10^{19}/s
Activation energy	1.97×10^{12} ergs/g-mol

The calculated temperature for a thermal explosion time of 15 μs is 818 K, which corresponds to a temperature increase of 525° C. This temperature increase is much higher than those calculated for the parallel/oblique experiments. Taking 116° C as the maximum calculated temperature increase for the parallel/oblique tests, the time required for an adiabatic explosion would be 2.4×10^8 s.

In addition, the strain rate (and temperature increase) may have been limited by the explosive sample sliding at one or both of the interfaces with the flyer plate and anvil. The surface of the glass anvil had a commercial polish finish of 10 fringes per inch, and the steel target plate had a machined surface finish with roughness of 16 μin rms. Any future tests should address the possibility of slippage at these interfaces. A suggested approach would be to increase the traction by surface roughening. Also, the anvil consisted of glass plies laminated together by polyvinyl butyryl plies. In order to avoid the possibility of shear localization occurring in the polyvinyl butyryl, a single piece of thick glass could be used.

The steel flyer plate used in our tests had a yield strength of about 0.5 GPa, but we did not see any evidence of yielding on the face of the recovered flyer plate. Such yielding, if present, would decrease the impact pressure by a small amount. In order to avoid this possibility, a hardened steel flyer plate should be used for future tests.

The most direct means of increasing the temperature of the explosive sample is to increase its strain rate by increasing the velocity of the impacting projectile, decreasing the sample thickness, or doing both. It is instructive to calculate the temperature increase that would be expected using the data of shot No. 26 and varying the impacting velocity and the explosive sample thickness over a range of explosive viscosities. The yield strength of the explosive is assumed to be 0.35×10^9 dynes/cm^2. Figures 5 and 6 show the calculated temperature increases for several sample thicknesses and impacting velocities.

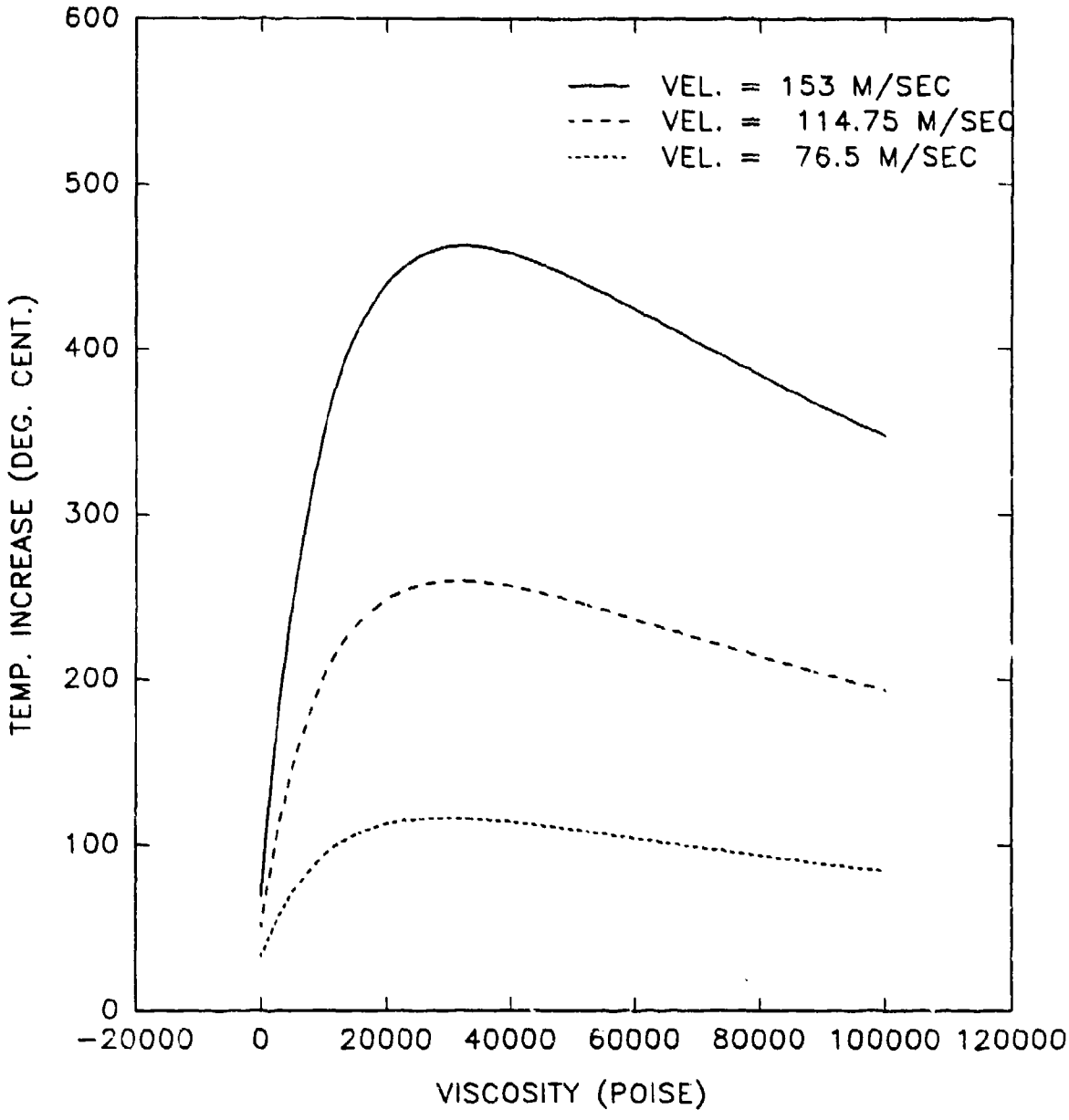

Figure 5. The temperature increase in an explosive target plotted as a function of the transverse component of the flyer plate velocity and the explosive viscosity. The sample thickness is 0.06 cm, and its yield strength is assumed to be 0.35 kbar.

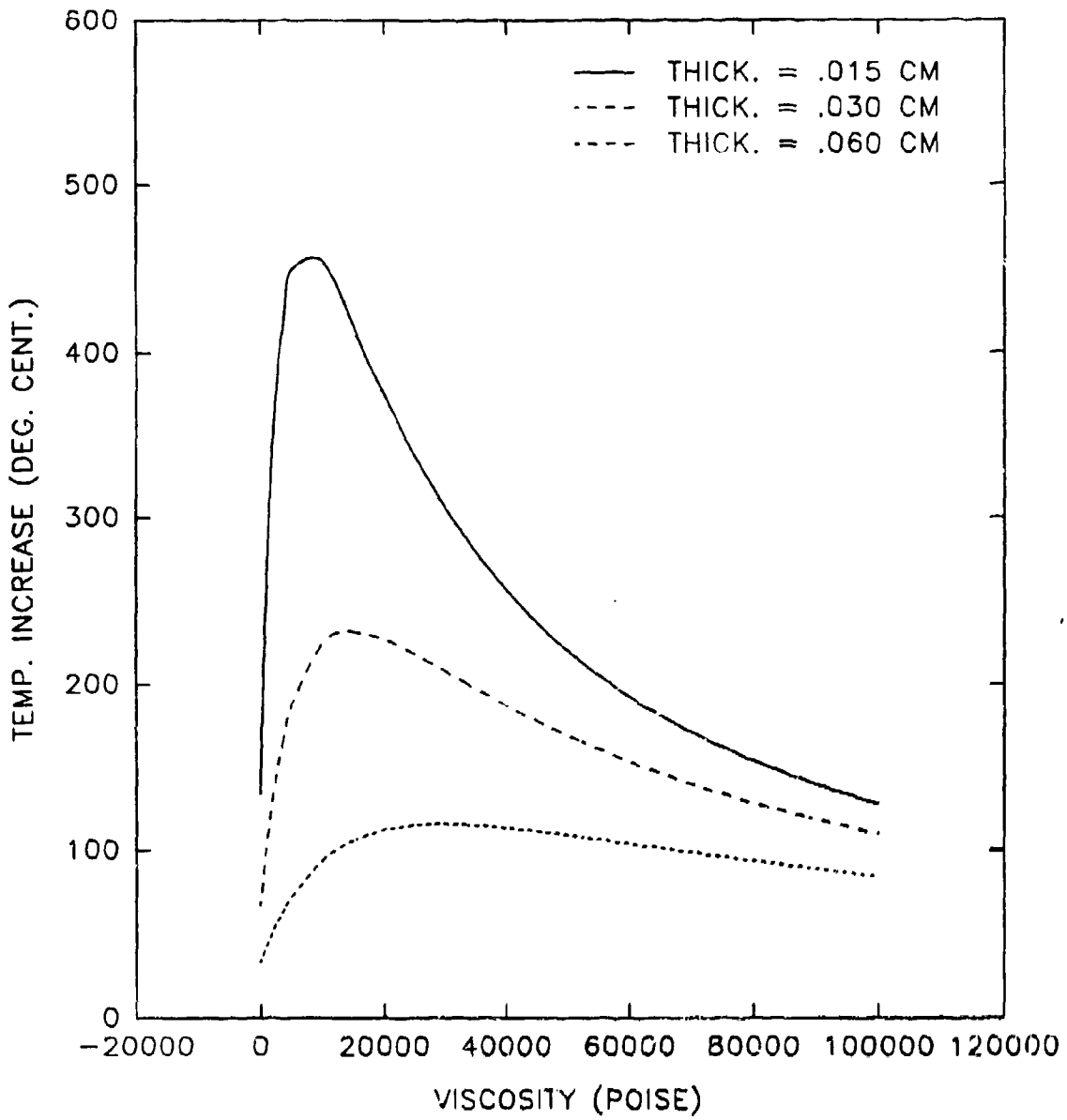

Figure 6. The temperature increase in an explosive target plotted as a function of the explosive thickness and viscosity. The transverse component of the flyer plate velocity is 7,650 cm/s, and the explosive yield strength is assumed to be 0.35 kbar.

5. Conclusions

We were not able to detect explosive reaction under conditions of combined pressure/shear. Using the experimental data and reasonable values for explosive yield strength and viscosity, we calculated a temperature increase of about 100° C in the impacted explosive. This increase in temperature is much too small to cause a thermal explosion in the time of our experiment, approximately 15 μs, and is also probably too small to generate observable reaction products.

Future tests of this type could be improved by using

(i) thicker explosive samples

(ii) higher gas velocities

(iii) thinned sections of the explosive interfaces

(iv) hardened flyer plates

(v) unpressurized gas gaps

INTENTIONALLY LEFT BLANK.

6. REFERENCES

Abou-Sayed, A. S., R. J. Clifton, and L. Hermann. "The Oblique-plate Impact Experiment." Experimental Mechanics, pp. 127–132, April 1976.

Boyle, V., R. Frey, and O. Blake. "Combined Pressure Shear Ignition of Explosives." Ninth Symposium (International) on Detonation, OCNR 113291-7, vol. 1, Portland, OR, 28 Aug–1 Sep 1989.

Halleck, P. M., and J. Wackerle. "Dynamic Elastic-Plastic Properties of Single Crystal Pentaerythritol Tetranitrate." Journal of Applied Physics, vol. 47, no. 3, 1976.

Kim, K. S., and R. J. Clifton. "Pressure-Shear Impact of 6061-T6 Aluminum." Journal of Applied Mechanics, vol. 47, pp. 11–16, March 1980.

Li, C. H., and R. J. Clifton. "Dynamic Stress-Strain Curves at Plastic Shear Strain Rates of 10^5 sec^{-1}." Shock Waves in Condensed Matter, AIP Conference Proceedings No. 78, edited by W. J. Nellis et al. Brown University, Providence, RI, 1981.

Pinto, J., S. Nicolaides, and D. A. Wiegand. "Dynamic and Quasi Static Mechanical Properties of Comp B and TNT." ARAED-TR-85004, U.S. Army Armament Research and Development Center, Dover, NJ, November 1985. (AD-E401419)

Rogers, R. N. "Thermochemistry of Explosives." Thermochimica Acta, vol. 2, 1975.

U.S. Army Materiel Command. Engineering Design Handbook - Principles of Explosive Behavior. AMCP 706-180, 1972.

INTENTIONALLY LEFT BLANK.

APPENDIX A:

DETAILS OF GAS GUN AND PROJECTILE

INTENTIONALLY LEFT BLANK.

The gas gun used for these tests was machined from 4140 steel and tempered to 35 on the Rockwell C scale. The barrel had the following basic dimensions:

length = 70 in
outside diameter = 7.750 in
bore diameter = 5.940 in.

A 1/4-in × 1/4-in × 70-in keyway was machined along the bore of the barrel in order to prevent rotation of the keyed projectile since rotation of projectiles having angled flyer plates could cause nonsimultaneous impact to occur. The gun had a wraparound breech of approximately 1,044-in^3 volume; the breech section was 24 in long and had an outside diameter of 14 in. The overall length of the assembled gun was 91 in. The total weight of the gun was about 1,500 lb.

The projectile consisted of a polyethylene body to which the flyer plate was bolted. It had the following characteristics:

body length = 12 in
body diameter = 5.925 in
flyer plate thickness = 2 in
flyer plate diameter = 5.75 in
total projectile weight = 15.4 lb to 22.9 lb.

The projectile had two O-rings (Parker 2-432) which served to seal against the high pressure nitrogen gas contained in the wraparound breech as shown in Figure A-1. When a small pressure is introduced through valve A, the projectile is displaced from its initial position and uncovers four large portholes connecting the wraparound breech to the gun bore. The high pressure breech gas which dumps behind the projectile causes it to accelerate rapidly. The O-rings were fitted against the gun bore with a 10% squeeze. For the tests reported here, the lowest velocity was obtained with a breech pressure of 125 psi and the highest with a breech pressure of 1,300 psi. We were not able to pressurize the breech beyond 1,300 psi due to leaks—probably past the O-rings.

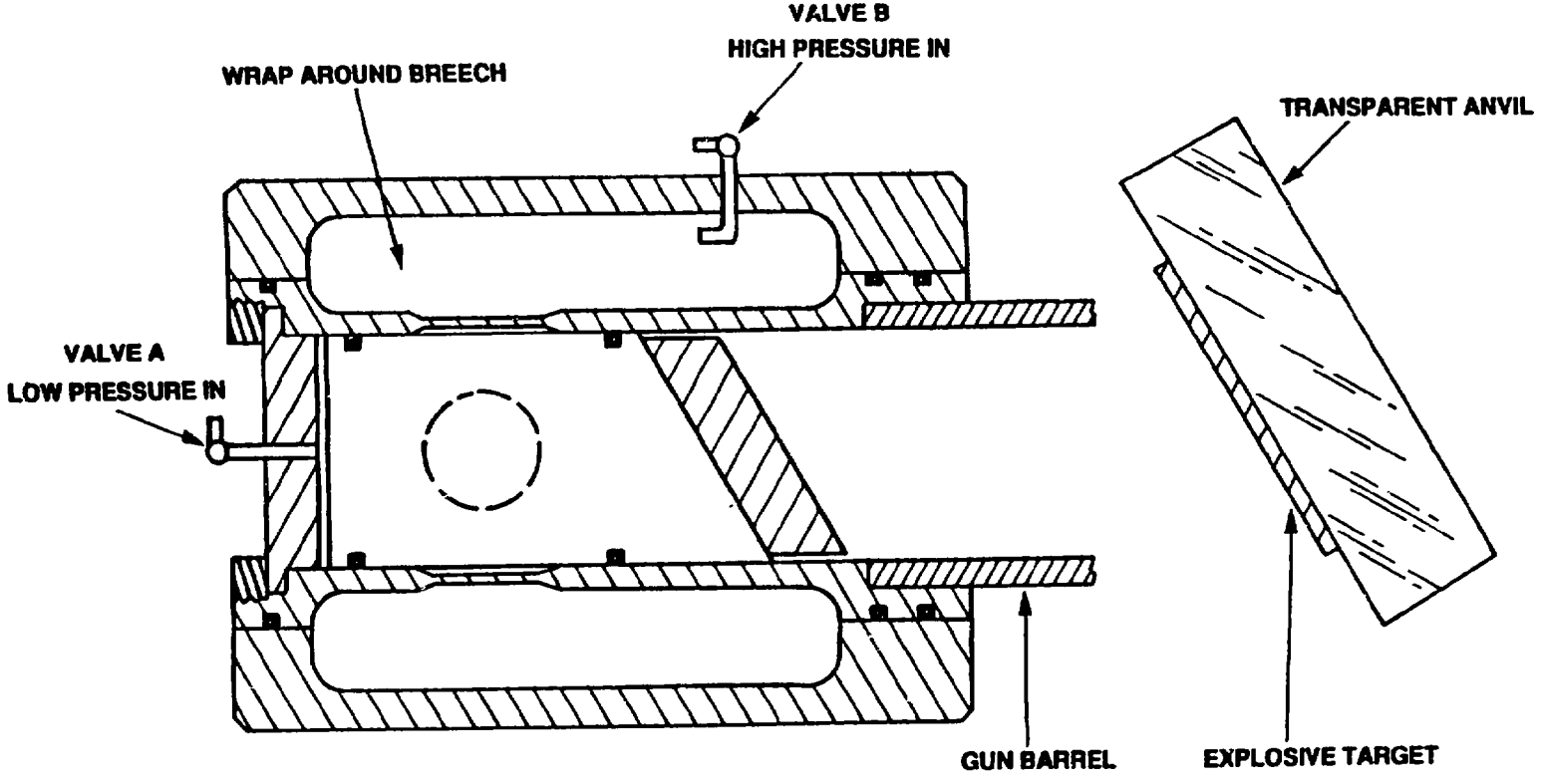

Figure A-1. Detail of the wraparound breech showing the gas seal provided by the O-rings on the projectile body.

APPENDIX B:

EVALUATION OF THE STRAIN RATE

INTENTIONALLY LEFT BLANK.

Notation:

S_1 = shear stress in projectile, dynes/cm^2

S_2 = shear stress in target (explosive), dynes/cm^2

S_3 = shear stress in anvil, dynes/cm^2

ν = viscosity of explosive, poise

Y = yield strength of explosive, dynes/cm^2

G_1 = shear modulus of projectile, dynes/cm^2

G_3 = shear modulus of anvil, dynes/cm^2

C_1 = elastic shear wave speed in projectile, cm/s

C_3 = elastic shear wave speed in anvil, cm/s

V_t = initial component projectile velocity parallel to the interface, cm/s

V_1 = component of projectile velocity parallel to the interface after impact, cm/s

V_3 = component of anvil velocity parallel to the interface after impact, cm/s

ε_1 = shear strain in the projectile, cm/cm

ε_3 = shear strain in the anvil, cm/cm

τ = thickness of the target plate, cm,

$\dot{\varepsilon}_2$ = shear strain rate in the target, s^{-1}

where

G_1 (steel) = 7.68×10^{11} dynes/cm^2

G_1 (alum.) = 2.78×10^{11} dynes/cm^2

G_3 (glass) = 2.65×10^{11} dynes/cm^2

C_1 (steel) = 3.12×10^5 cm/s

C_1 (alum.) = 3.16×10^5 cm/s

C_3 (glass) = 3.45×10^5 cm/s.

To evaluate the strain rate in the target, we make the following assumptions:

(1) After a few reverberations of the wave back and forth across the target layer, the shear in the target plate is homogeneous; i.e., there is no strain localization. This assumption gives the lowest possible strain rate. We will analyze this situation and will not consider the transient that exists before the homogeneous state is attained.

(2) The stress and particle velocity are continuous at the interfaces.

(3) The projectile and the anvil respond elastically, so that

$$S_1 = G_1\varepsilon_1 \tag{B1}$$

and

$$S_3 = G_3\varepsilon_3 \,. \tag{B2}$$

(4) The explosive obeys the following very simple constitutive relation:

$$S_2 = Y + \nu\,\dot{\varepsilon}_2 = Y + \nu\,(V_1 - V_3)\,/\,\tau \,. \tag{B3}$$

We recognize that real materials will have more complex behavior.

(5) We ignore heating of the layer and variations in the viscosity or the yield strength with temperature.

With these assumptions, the transverse velocity (the component parallel to the interfaces) varies as shown schematically in Figure B-1. A shock moves back into the projectile and reduces its transverse velocity from V_t to V_1. A shock moves to the right in the anvil and increases its transverse velocity from 0 to V_3. Within the target layer, the velocity varies linearly from V_1 to V_3. The shear strain in the anvil is

$$\varepsilon_3 = \frac{V_3}{C_3} \,. \tag{B4}$$

The shear strain in the projectile is

$$\varepsilon_1 = \frac{V_t - V_1}{C_1} \,. \tag{B5}$$

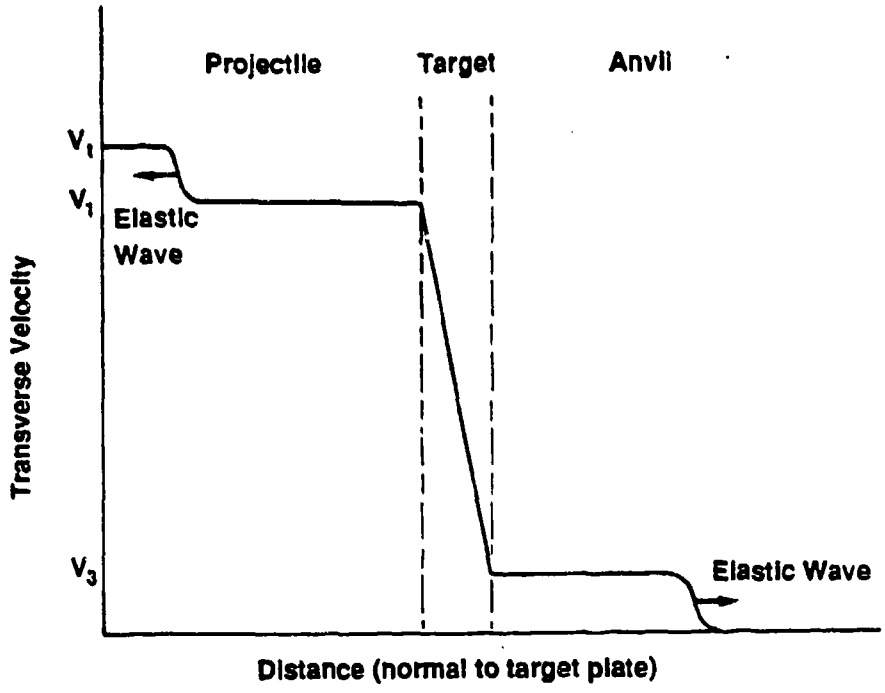

Figure B-1. The transverse velocity (the component parallel to the interfaces) in the flyer plate, explosive target, and the anvil after impact.

The shear strain rate in the target is

$$\dot{\varepsilon}_2 = (V_1 - V_3) / \tau \, . \tag{B6}$$

At the interfaces, the stress is continuous, so the following equations hold:

$$G_1 (V_t - V_1) / C_1 = \nu (V_1 - V_3) / \tau + Y \, , \tag{B7}$$

and

$$G_3 (V_3) / C_3 = \nu (V_1 - V_3) / \tau + Y \, . \tag{B8}$$

Solving for V_1 and V_3 gives the following result:

$$V_1 = \left(\frac{G_1}{C_1} V_1 - Y + \frac{G_1}{C_1}\frac{C_3}{G_3}\frac{\nu}{\tau} V_1\right) \Big/ \left(\frac{G_1}{C_1} + \frac{\nu}{\tau} + \frac{G_1}{C_1}\frac{C_3}{G_3}\frac{\nu}{\tau}\right). \tag{109}$$

and

$$V_3 = \frac{G_1}{C_1}(V_1 - V_1)\frac{C_3}{G_3}. \tag{110}$$

The viscosity is unknown for the explosives that we used (and the constitutive relation used here is almost certainly too simple to represent a real material). Nevertheless, we can make some guesses about the viscosity and calculate the resulting strain rate. Hallock and Wackerle[1] determined a viscosity for PETN of 50,000 poise in a shock wave experiment. This could be used as an upper bound. The yield strength under pressure is also not well known. It is clear that the yield strength under pressure is greater than the strength that is measured in unconfined uniaxial experiments.[2] Pinto, Nicolaides, and Wiegand[2] determined a yield strength for composition B of about 0.35 kbar. Using these values of viscosity and yield strength for Detasheet, we can calculate a strain rate, from equations B4 B10, and a temperature, equation 5, for experiment 26. The computed temperature increase that would be achieved in 19 μs is 95° C. Figure 4 shows the computed temperature increase for a range of viscosities and yield strengths. It can be seen that if yield strength is held constant, there is a viscosity value which gives the highest possible temperature.

---

[1] Hallock, P. M., and J. Wackerle "Dynamic Elastic Plastic Properties of Single Crystal Pentaerythritol Tetranitrate" Journal of Applied Physics, vol 47, no 3, 1976

[2] Pinto, J., R. Nicolaides, and D. A. Wiegand "Dynamic and Quasi-Static Mechanical Properties of Comp B and PBX ARAED TR-85004, U.S. Army Armament Research and Development Center, Dover, NJ, November 1985 (AD B096319).

[redacted]

[redacted]

INTENTIONALLY LEFT BLANK.

We can calculate the impact pressure produced when a flyer plate strikes an anvil. We assume that the impact remains elastic. After impact, the pressure in the flyer plate and the anvil are equal at the interface and the interface has a common particle velocity. The following notation applies:

V_n = normal component of flyer plate velocity, cm/s
u_i = interface particle velocity, cm/s
ρ_a = density of anvil, g/cm^3
ρ_f = density of flyer plate, g/cm^3
U_a = elastic longitudinal wave speed in anvil, cm/s
U_f = elastic longitudinal wave speed in flyer plate, cm/s
P_a = pressure in anvil, dynes/cm^2
P_f = pressure in flyer plate, dynes/cm^2
P_i = interface pressure, dynes/cm^2
P_x = pressure in explosive, dynes/cm^2.

After impact, an elastic wave of velocity U_a propagates into the anvil and an elastic wave of velocity U_f propagates into the flyer plate. The anvil undergoes a change in particle velocity ($u_i - 0$), and the flyer plate particle velocity undergoes a change ($V_n - u_i$). By the laws of conservation of mass and momentum across the elastic wave, we can write:

$$P_a = \rho_a U_a (u_i - 0) \text{ and } P_f = \rho_f U_f (V_n - u_i) . \tag{C1}$$

At the interface $P_a = P_f$. Therefore we can write:

$$\rho_a U_a u_i = \rho_f U_f (V_n - u_i).$$

This can be solved for u_i:

$$u_i = \rho_f U_f V_n / (\rho_a U_a + \rho_f U_f) . \tag{C2}$$

Then, since we assumed that $P_x = P_i = P_f = P_a$ we can write:

$$P_x = P_a = \rho_a U_a \rho_f U_f V_n / (\rho_a U_a + \rho_f U_f) . \tag{C3}$$

The impact of the flyer plate on the anvil is illustrated in Figure C-1, which shows the elastic equation of state in the pressure-particle velocity plane.

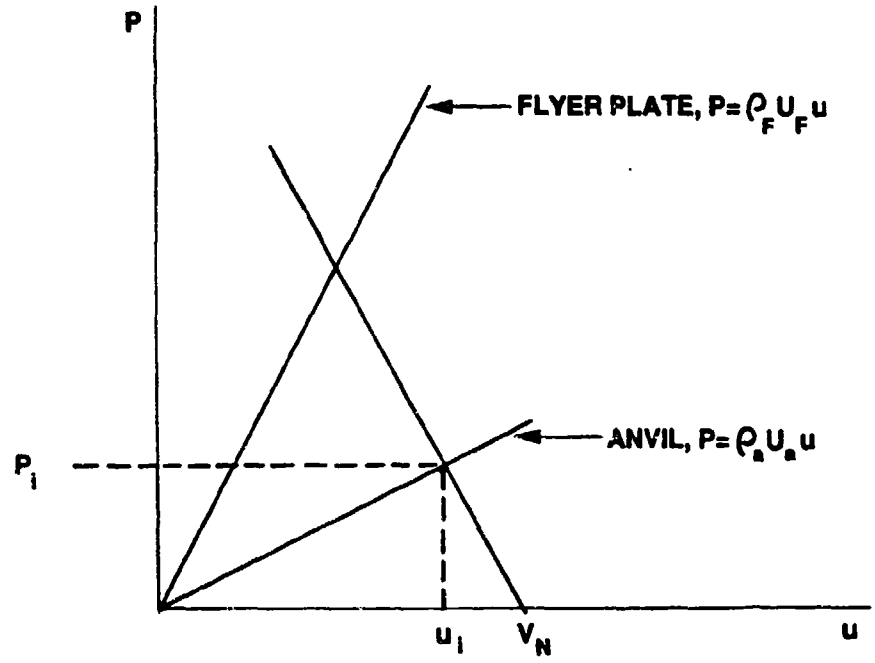

Figure C-1. The elastic impact of the flyer plate on the anvil is shown in the pressure-particle velocity plane.

No. of Copies	Organization
2	Administrator Defense Technical Info Center ATTN: DTIC-DDA Cameron Station Alexandria, VA 22304-6145
1	Commander U.S. Army Materiel Command ATTN: AMCAM 5001 Eisenhower Ave. Alexandria, VA 22333-0001
1	Director U.S. Army Research Laboratory ATTN: AMSRL-OP-SD-TA, Records Management 2800 Powder Mill Rd. Adelphi, MD 20783-1145
3	Director U.S. Army Research Laboratory ATTN: AMSRL-OP-SD-TL, Technical Library 2800 Powder Mill Rd. Adelphi, MD 20783-1145
1	Director U.S. Army Research Laboratory ATTN: AMSRL-OP-SD-TP, Technical Publishing Branch 2800 Powder Mill Rd. Adelphi, MD 20783-1145
2	Commander U.S. Army Armament Research, Development, and Engineering Center ATTN: SMCAR-TDC Picatinny Arsenal, NJ 07806-5000
1	Director Benet Weapons Laboratory U.S. Army Armament Research, Development, and Engineering Center ATTN: SMCAR-CCB-TL Watervliet, NY 12189-4050
1	Director U.S. Army Advanced Systems Research and Analysis Office (ATCOM) ATTN: AMSAT-R-NR, M/S 219-1 Ames Research Center Moffett Field, CA 94035-1000

No. of Copies	Organization
1	Commander U.S. Army Missile Command ATTN: AMSMI-RD-CS-R (DOC) Redstone Arsenal, AL 35898-5010
1	Commander U.S. Army Tank-Automotive Command ATTN: AMSTA-JSK (Armor Eng. Br.) Warren, MI 48397-5000
1	Director U.S. Army TRADOC Analysis Command ATTN: ATRC-WSR White Sands Missile Range, NM 88002-5502
1	Commandant U.S. Army Infantry School ATTN: ATSH-WCB-O Fort Benning, GA 31905-5000
	Aberdeen Proving Ground
2	Dir, USAMSAA ATTN: AMXSY-D AMXSY-MP, H. Cohen
1	Cdr, USATECOM ATTN: AMSTE-TC
1	Dir, USAERDEC ATTN: SCBRD-RT
1	Cdr, USACBDCOM ATTN: AMSCB-CII
1	Dir, USARL ATTN: AMSRL-SL-I
5	Dir, USARL ATTN: AMSRL-OP-AP-L

No. of Copies	Organization
1	HQDA (SARD-TR/Ms. K. Kominos) WASH DC 20310-0103
1	HQDA (SARD-TR/Dr. R. Chait) WASH DC 20310-0103
1	Administrator Lockheed Missiles and Space Co. Org. 89–10, Bldg. 157 ATTN: Y. Choo Sunnyvale, CA 94088-3504
	Aberdeen Proving Ground
8	Dir, USARL ATTN: AMSRL-WT-T, T. Wright AMSRL-WT-TB, F. Gregory W. Hillstrom O. Lyman J. Watson J. Starkenberg AMSRL-WT-TD, J. Walter AMSRL-WT-PE, D. Kooker

USER EVALUATION SHEET/CHANGE OF ADDRESS

This Laboratory undertakes a continuing effort to improve the quality of the reports it publishes. Your comments/answers to the items/questions below will aid us in our efforts.

1. ARL Report Number ARL-TR-584 Date of Report October 1994

2. Date Report Received _____

3. Does this report satisfy a need? (Comment on purpose, related project, or other area of interest for which the report will be used.) _____

4. Specifically, how is the report being used? (Information source, design data, procedure, source of ideas, etc.) _____

5. Has the information in this report led to any quantitative savings as far as man-hours or dollars saved, operating costs avoided, or efficiencies achieved, etc? If so, please elaborate. _____

6. General Comments. What do you think should be changed to improve future reports? (Indicate changes to organization, technical content, format, etc.) _____

CURRENT ADDRESS

_____
Organization

_____
Name

_____
Street or P.O. Box No.

_____
City, State, Zip Code

7. If indicating a Change of Address or Address Correction, please provide the Current or Correct address above and the Old or Incorrect address below.

OLD ADDRESS

_____
Organization

_____
Name

_____
Street or P.O. Box No.

_____
City, State, Zip Code

(Remove this sheet, fold as indicated, tape closed, and mail.)
(DO NOT STAPLE)